

# Characterization of Ga-substituted zeolite Beta by X-ray absorption spectroscopy

Carlos Prieto,<sup>a</sup> Teresa Blasco,<sup>b</sup> Miguel Cambor<sup>b</sup> and Joaquin Pérez-Pariente<sup>b</sup>

<sup>a</sup>Instituto de Ciencia de Materiales de Madrid, Consejo Superior de Investigaciones Científicas, Cantoblanco, 28049 Madrid, Spain

<sup>b</sup>Instituto de Tecnología Química, Consejo Superior de Investigaciones Científicas-Universidad Politécnica de Valencia, Avda de los Naranjos s/n, 46022 Valencia, Spain

Received 29th February 2000, Accepted 28th March 2000

Published on the Web 11th May 2000

The incorporation of Ga into the framework of zeolite Beta has been evidenced by X-ray absorption spectroscopy. Analysis of extended X-ray absorption fine structure (EXAFS) and X-ray absorption near edge structure (XANES) data reveals the atomic environment of Ga in zeolite Beta. Both techniques provide evidence that calcination and dehydration of the synthesized zeolites provokes changes in the Ga atomic environment, which can be understood as due to the migration of Ga from framework sites to extra-framework positions. The XANES results allow calculation of the atomic fraction at both positions.

## I Introduction

The isomorphous substitution of silicon or aluminium by other elements in zeolites is of great interest from a catalytic point of view. Since metal cations can act as active centers in some catalytic reactions, the incorporation of other elements into the network strongly influences the catalytic properties of the material. In addition to this, the presence of other atoms can also modify the acidic properties of the zeolite. Gallium-containing zeolites incorporate both basic and acidic centers, which is related to the co-existence of tetrahedral and octahedral Ga species within such materials. This property has been proven to be relevant<sup>1</sup> for methanol conversion,<sup>2</sup> hydrocarbon cracking<sup>3</sup> and conversion of light alkanes.<sup>4</sup>

Zeolite Beta is a twelve-membered ring zeolite with a large pore structure, such that molecules of up to 6.5 Å can interact with the active sites located in the pores. A complete structural characterization of zeolite Beta has been reported by Newsam *et al.*<sup>5</sup> Isomorphous substitution of Si or Al by other elements, such as B, Ga and Ti, has been achieved previously.<sup>6–8</sup> In the present work, we show that Ga atoms are in framework positions in zeolite Beta and that, after calcination and dehydration, some of them relocate from the zeolite network to extra-framework positions.

The incorporation of Ga in zeolites has been studied by several authors using various techniques, such as solid state NMR, XRD and IR, to show that Ga<sup>3+</sup> may replace Si<sup>4+</sup> in ZSM-11<sup>9</sup> and ZSM-5,<sup>10,11</sup> as well as to investigate the influence of this substitution on the lattice crystallinity and defect sites.<sup>12</sup> The Brønsted acidity in [Si,Ga]ZSM-5 has been related to the presence of four-coordinate gallium, which is the structural origin of the catalytic activity of this zeolite.<sup>13</sup> A very interesting study on the characterization of gallosilicates by IR spectroscopy of adsorbed probe molecules has been reported; this work found that samples with different thermal preparation display either Brønsted or Lewis acidic character depending on the partial or total extra-framework position of Ga<sup>3+</sup> ions.<sup>14</sup>

Direct evidence for the incorporation of Ga into the zeolite framework requires the use of convenient spectroscopic techniques. X-Ray absorption spectroscopy (XAS) has proven to be a powerful tool to study the local environment of metal cations in zeolites,<sup>15–17</sup> it can be very useful to gain some insight into the coordination environment of Ga. Two

different sets of information can be obtained by using the same experimental XAS set-up: X-ray absorption near edge structure (XANES) is related to oxidation state and the stereochemical coordination of the absorbing atoms and extended X-ray absorption fine structure (EXAFS) gives the radial distribution function around these atoms. In a pioneering investigation, Axon *et al.*<sup>18</sup> used EXAFS spectroscopy to study Ga-substituted MFI-type zeolites. In this work, a tetrahedral coordination mode is proposed for a sample after calcination and dehydration. The reported coordination number is bigger than four, which, alternatively, could be explained by considering a mixture of tetrahedral and octahedral gallium with very similar distances.

## II Experimental

The synthesis mixture for the Ga Beta zeolite was prepared using amorphous silica (Aerosil 200, Degussa) tetraethylammonium hydroxide (40 wt%, aqueous solution, K < 1 ppm, Na < 3 ppm, Alfa), aluminium nitrate nonahydrate (95%, Merck) and gallium and germanium oxides (Alfa).

Gels of appropriate oxide molar composition:  $x\text{SiO}_2 : y\text{Ga}_2\text{O}_3 : z(\text{GeO}_2 \text{ or } \text{Al}_2\text{O}_3) : 18.5(\text{TEA})_2\text{O} : 750\text{H}_2\text{O}$  were prepared and introduced into 60 ml PTFE-lined stainless-steel autoclaves, stirred at 60 rpm and heated at 408 K for 10 days. The solid products were recovered by centrifugation, washed until the pH reached 9 and dried at 353 K overnight. The chemical compositions of the samples (atoms per unit cell) were 58Si : 3Ga : 3Ge (hereafter referred to as GaGe-ZEOL) and 58Si : 5Ga : 1Al (hereafter denoted GaAl-ZEOL). Calcined samples were obtained by heating the crude crystals in air at 853 K for 3 h. Then, a portion of each sample was dehydrated by heating for 5 h under flowing nitrogen at 250 °C. Special care was taken with the dehydrated samples, they were stored under a nitrogen atmosphere, transferred to the measuring chamber under an argon atmosphere and measured under vacuum conditions. The three preparations for each zeolite will be referred to as the “as-prepared”, “calcined” and “dehydrated” samples.

X-Ray absorption experiments were carried out at the XAS-3 beamline of the DCI storage ring (Orsay) with an electron beam energy of 1.85 GeV and an average current of 250 mA. Data were collected using a fixed exit monochromator

with two flat Si(311) crystals; the detector consisted of two ion chambers with air fill gas. The opening of the final slit was 0.4 mm, which gives an energy resolution of about 2 eV. Although the energy range is different for Ga and Cu, the resolution was estimated to be similar to that obtained for Cu foil by measuring the 3d near edge feature. Typically, two or three spectra were collected for averaging with a sampling step and acquisition time per point of 0.4 eV/0.5 s and 2.0 eV/1.0 s for XANES and EXAFS spectra, respectively.

### III Results and discussion

#### (a) EXAFS spectroscopy

EXAFS experiments were performed on the compounds at the Ga K-edge. A standard analysis of the EXAFS oscillations has been performed by using a PC computer program developed by Bonnin *et al.*<sup>19</sup> The  $\chi(k)$  EXAFS signal was obtained after subtraction of the atomic background, which is fitted by a cubic spline polynomial. Fig. 1 shows the  $k^3$ -weighted EXAFS signal of the studied samples. The corresponding pseudo radial distribution function (RDF) was calculated weighting  $\chi(k)$  by the cubic wavenumber ( $k^3$ ), multiplying by a Hanning window and Fourier transforming. The magnitudes of the Fourier transform (FT) are shown in Fig. 2. In order to allow comparison between samples, the  $k$ -interval for the Fourier transform has been kept constant from 2.0 to 13.75  $\text{\AA}^{-1}$ . The first peak (centered at 1.6  $\text{\AA}$ ) is related to Ga–O distances. Due to the fact that this peak is separated from the other contributions, it is possible to analyze it separately.

In order to obtain accurate Ga–O distances and coordination numbers, EXAFS oscillations were fitted to the well-known expression:<sup>20</sup>

$$\chi(k) = S_0^2 \sum_j \frac{N_j}{kR_j^2} \times e^{-2k^2\sigma_j^2} \times e^{-\frac{\Gamma_j}{k}} \times f_j(k) \times \sin[2kR_j + \phi_j(k)] \quad (1)$$

Eqn. (1) describes the EXAFS oscillations for a Gaussian distribution of  $N_j$  atoms at mean distances  $R_j$  around the absorbing atom, considering single scattering and plane-wave approximations.  $S_0^2$  is an intrinsic loss factor,  $N_j$  is the average coordination number for the Gaussian distribution of distances centered at the  $R_j$  value,  $\sigma_j$  is the Debye–Waller (DW) factor, and  $\phi_j(k) = 2\delta(k) + \gamma_j(k)$  is the phase shift;  $\delta(k)$  and  $\gamma_j(k)$  being the central and backscattering atom phase shifts, respectively.  $f_j(k)$  is the magnitude of the backscattering amplitude of the  $j^{\text{th}}$

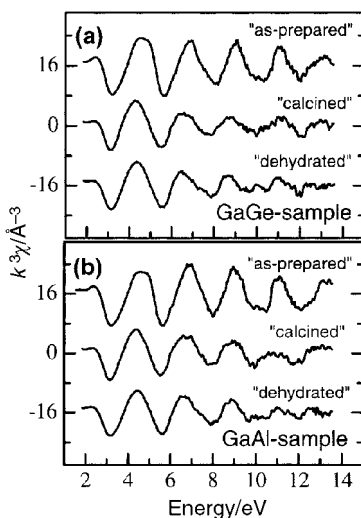


**Fig. 1**  $k^3$ -Weighted EXAFS signals of the two studied Ga-substituted zeolite Beta samples. (a) GaGe-ZEOL sample (unit cell: 58Si: 3Ga: 3Ge); (b) GaAl-ZEOL sample (unit cell: 58Si: 5Ga: 1Al). Spectra have been shifted vertically for the sake of clarity.

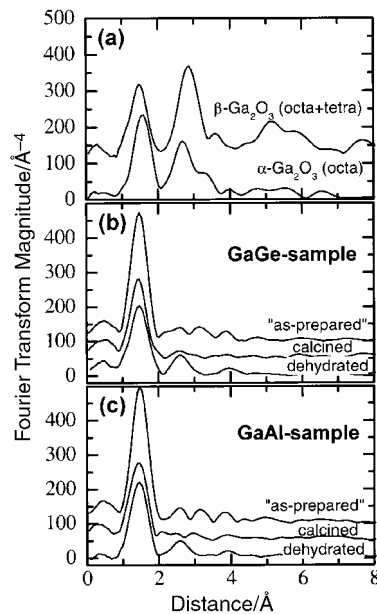


**Fig. 2** Fourier transform magnitude corresponding to the Ga K-edge EXAFS signals from reference compounds and samples shown in Fig. 1.

neighbour atom, and  $k/\Gamma_j$  is a convolution of the mean free path of the photoelectron travelling from the absorbing atom to the backscatter in the  $j^{\text{th}}$  shell and the life time of the core hole.

In order to study the substitution of Ga ions into framework or extra-framework positions in Beta zeolite, two possible atomic environments should be considered, *i.e.* tetrahedral and octahedral, for that foreign ion. Zeolite framework sites should have tetrahedral symmetry, as do the silicon or aluminium constituent atoms, and extra-framework positions are expected to have an octahedral environment, because that corresponds to a position between two tetrahedra. We have used two Ga oxides as reference compounds, but it has not been possible for us to obtain an isolated octahedral environment reference. The alternative is to calculate the backscattering functions for such an environment, using the FEFF code,<sup>21</sup> then fit the known references to check them and, finally, fit the unknown Ga-containing zeolite Beta samples.

The Ga–O references used were the  $\alpha$ - and  $\beta$ -phases of  $\text{Ga}_2\text{O}_3$ . The  $\alpha$ -phase is the hydrated form of  $\text{Ga}_2\text{O}_3$ , which belongs to the  $R\bar{3}c$  space group, having a sixfold octahedral environment with three Ga–O distances of 2.08  $\text{\AA}$  and three others of 1.92  $\text{\AA}$  in the  $\text{GaO}_6$  octahedra.<sup>22</sup> In order to fit this sample, the Ga–O backscattering phase and amplitude functions were calculated using the FEFF6.01 code.<sup>23</sup>  $\alpha$ - $\text{Ga}_2\text{O}_3$  was considered to be a cluster with an octahedral oxygen environment at a distance of 2.0  $\text{\AA}$ . The results of the fits are given in Table 1, from these, the inelastic loss factors,  $S_0^2$ , can be used to fit the other samples with octahedral environments.

A second Ga reference was also employed;  $\beta$ - $\text{Ga}_2\text{O}_3$  presents a  $C2/m$  space group structure,<sup>24</sup> in which one half of the Ga atoms are in an octahedral environment with two averaged distances of 1.95 and 2.06  $\text{\AA}$  and the other half are in a tetrahedral environment with a mean Ga–O distance of 1.83  $\text{\AA}$ . Two clusters were used to simulate this mixed environment: the previous octahedral reference and a tetrahedral cluster with Ga–O distances of 1.83  $\text{\AA}$ . In this way, we obtained the  $S_0^2$  factors for both environments; we considered these factors to remain constant when using them to fit the zeolite samples.

We will concentrate on the peak centered at 1.6  $\text{\AA}$  for every sample. Looking at the FT magnitude in Fig. 2 for the GaGe-ZEOL and GaAl-ZEOL samples, the first observation that can

**Table 1** EXAFS parameters of the reference compounds and the two Ga-substituted zeolite Beta samples studied: GaGe-ZEOL (unit cell: 58 Si : 3 Ga : 3Ge) and GaAl-ZEOL (unit cell: 58 Si : 6 Ga : 1Al). Asterisks indicate values which have been taken from the reported crystallographic data and numbers in parentheses are the experimental error in the last digit. The last column lists the tetrahedral and octahedral site percentages calculated by fitting the XANES spectra to the linear combination discussed in the text

Sample	Bond	$R/\text{\AA}$	$N(\text{fit})$	$\sigma/\text{\AA}$	$S_0^2$	$\Delta R/\text{\AA}$	$N(\text{actual})$	% tetra and octa (XANES)
$\alpha$ -Ga <sub>2</sub> O <sub>3</sub> (octa)	Ga–O(octa)	1.91*, 2.03*	2.51*	0.06(1)	0.84(3)	1.10	3.0	100 (octa)*
$\beta$ -Ga <sub>2</sub> O <sub>3</sub> (tetra + octa)	Ga–O(tetra)	1.84*	2.12*	0.06(1)	1.06(8)	1.10	2.0	50 (tetra)*
	Ga–O(octa)	1.91*, 2.03*	1.25*	0.06(1)	0.84(3)		1.5	50 (octa)*
GaGe-ZEOL (as-prepared)	Ga–O(tetra)	1.80(1)	3.8(1)	0.05(1)		0.98	3.6	100 (tetra)*
	Ga–O(octa)	—	0	—			0	
GaGe-ZEOL (calcined)	Ga–O(tetra)	1.80(1)	1.3(2)	0.04(1)		1.04	1.2	55 (tetra)
	Ga–O(octa)	1.83(1), 1.98(1)	1.5(1)	0.04(1)			1.8	45 (octa)
GaGe-ZEOL (dehydrated)	Ga–O(tetra)	1.80(1)	0.9(5)	0.06(1)		1.23	0.9	75 (tetra)
	Ga–O(octa)	1.82(2), 1.94(1)	1.5(5)	0.06(1)			1.8	25 (octa)
GaAl-ZEOL (as-prepared)	Ga–O(tetra)	1.80(1)	4.1(3)	0.05(1)		1.10	3.9	100 (tetra)*
	Ga–O(octa)	—	0	—			0	
GaAl-ZEOL (calcined)	Ga–O(tetra)	1.83(1)	3.4(3)	0.08(1)		1.04	3.2	55 (tetra)
	Ga–O(octa)	1.75(5), 2.03(3)	0.4(1)	0.08(1)			0.5	45 (octa)
GaAl-ZEOL (dehydrated)	Ga–O(tetra)	1.83(1)	3.4(3)	0.08(1)		1.04	3.2	75 (tetra)
	Ga–O(octa)	1.75(3), 2.03(3)	0.4(1)	0.08(1)			0.5	25 (octa)

be made is that the peak magnitude for the “as-prepared” samples is much greater than those for both the Ga<sub>2</sub>O<sub>3</sub> oxides. As a qualitative consideration, this can be explained by the fact that the Ga atoms in the GaGe-ZEOL and GaAl-ZEOL samples are in a more ordered environment than in the reference oxides. This ordered environment should be a regular GaO<sub>4</sub> tetrahedron, which increases the FT magnitude, since the distances to the four surrounding oxygen atoms will be identical. In comparison, the octahedral GaO<sub>6</sub> environment in  $\alpha$ -Ga<sub>2</sub>O<sub>3</sub> has two different Ga–O distances, which decreases the FT magnitude.

In order to analyze these peaks, we have considered three different distances in the fitting procedure. One is associated with the tetrahedral environment, with only one value for the GaO<sub>4</sub> distances, and the other two are associated with the octahedral environment, in which there is the possibility of having two different values for the GaO<sub>6</sub> distances (as in the case of the  $\beta$ -phase reference oxide). It should be mentioned that there are several constraints between the three shell parameters which ensures that the maximum number of independent parameters provided by the Nyquist theorem is not exceeded for any sample (this number can be calculated from  $N_{\text{idp}} = 2\Delta k \Delta R / \pi$ ).<sup>25</sup> The obtained  $N_{\text{idp}}$  was greater than or equal to 9 (except for the “as-prepared” GaGe-ZEOL sample, where  $N_{\text{idp}} = 8.2$ ) and the maximum number of fitted parameters was never more than 7 (3 distances, 1 DW factor, 2 coordination numbers and 1 energy shift factor), the only constraint imposed among the parameters is that we have taken equal DW factors for tetrahedral and octahedral environments.

The results of the analysis procedure are summarized in Table 1. It was found that, in the “as-prepared” GaGe-ZEOL and GaAl-ZEOL samples, Ga exists in the tetrahedral environment only. This can be explained by the fact that all the Ga atoms are inside the Beta zeolite framework structure, with Ga–O distances of 1.80 Å. This value lies between that for the GaO<sub>4</sub> tetrahedra in  $\alpha$ -Ga<sub>2</sub>O<sub>3</sub> (1.83 Å) and the Si–O (1.61 Å) and Al–O (1.72 Å) distances reported in ref. 5; it seems that the Beta zeolite structure imposes a reduction in the Ga ionic radius, but local order around Ga also becomes slightly deformed. On the other hand, the obtained Ga–O distances are in full agreement with that obtained from gallosilicate sodalite by powder neutron diffraction.<sup>26</sup> The EXAFS spectra change after calcination and dehydration, the analysis gives a mixed environment for Ga atoms in both samples after thermal treatments. This can be explained by the migration of some tetrahedrally coordinated Ga atoms (framework sites) to octahedral environments (extra-framework positions) with Ga–O distances near 1.8 and 2.0 Å. The results for both the GaGe-ZEOL and GaAl-ZEOL samples are similar and are in

agreement with the degallation during calcination of Ga-MFI Zeolite observed by <sup>29</sup>Si MAS-NMR studies.<sup>10</sup>

In principle, the ratio between the actual and the maximum possible coordination number for each environment could be related to the relative percentages of the framework and extra-framework positions, but the numbers of oxygen vacancies in both environments are unknown. This fact would result in an erroneous determination of the relative percentages.

### (b) XANES spectroscopy

In addition to the EXAFS spectroscopy, XANES spectra have been used to confirm the above conclusions. Fig. 3 shows the XANES spectra of the as-prepared, calcined and dehydrated Ga-containing zeolite Beta samples. The spectra of the reference oxides are also given, including that for GeO<sub>2</sub> quartz, which provides a XANES spectrum for tetrahedrally coordinated Ge; a very similar spectrum can be expected for the equally four-coordinate Ga environment in the zeolite samples.

First of all, we should understand the XANES spectra of the two Ga<sub>2</sub>O<sub>3</sub> references. The octahedral environment of Ga in

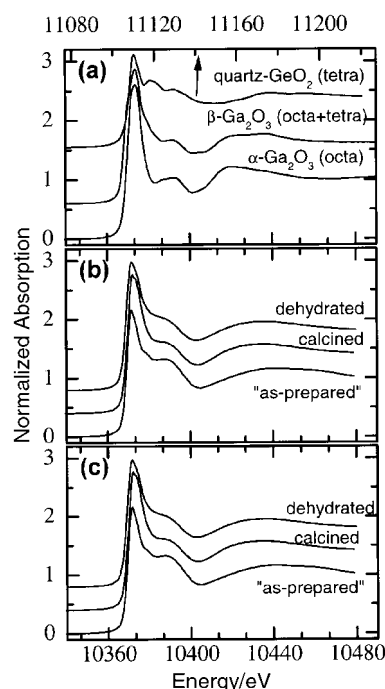


**Fig. 3** Normalized XANES spectra: (a) reference compounds; (b) GaGe-ZEOL samples; (c) GaAl-ZEOL samples.

$\alpha$ -Ga<sub>2</sub>O<sub>3</sub> gives a XANES spectrum that can be described as a narrow “white line” (10373 eV) and a feature at 10393 eV. Nevertheless, the mixed environment of Ga in  $\beta$ -Ga<sub>2</sub>O<sub>3</sub> gives a wider “white line” (10373 eV) with two shoulders at lower and higher energies than the maximum (10370 and 10379.5 eV) and a feature at 10393 eV, the same energy as for the  $\alpha$ -phase. In view of the fact that the XANES spectrum of tetrahedrally coordinated Ga should be similar to that for quartz-GeO<sub>2</sub>, the  $\beta$ -Ga<sub>2</sub>O<sub>3</sub> XANES spectrum can be easily interpreted as a sum of two spectra corresponding to the octahedral and tetrahedral environments, where the feature at 10379.5 eV cannot be readily resolved. The two features at 10373 and 10379.5 eV are in agreement with the literature-reported spectrum of tetrahedrally coordinated Ga in the gallosilicate sodalite Na-SOD-GaSi, for which there are two big maxima at these energies in its XANES spectrum.<sup>27</sup>

In principle, it is reasonable to assume that the broadening of the white line is due to the existence of the two Ga environments. The evolution of the XANES spectra of the Beta zeolite samples can be analyzed as resulting from a sum of the spectra for both environments. A similar analysis has been performed by a combination of both tetrahedral and octahedral Ge environments. Itié *et al.* have performed studies on the phase transition under high pressure of GeO<sub>2</sub><sup>28</sup> and various other compounds, such as MGeO<sub>3</sub> pyroxenoid<sup>29</sup> and M<sub>2</sub>GeO<sub>4</sub> olivine (with M=Mg or Ca).<sup>30</sup> This permits the association of the appearance of the shoulders in the zeolite spectra with the existence of tetrahedrally coordinated Ga in the samples and enables estimation of the relative percentages of both environments. A similar analysis has been reported for several gallium coordination environments in oxides by simulation of the XANES spectrum, using two sets of Gaussian and arc tangent functions to take into account the two gallium environments.<sup>31</sup> It should be noted that our linear combination fit is extended to the whole XANES spectrum (a range of 80 eV), whereas the simulations performed by Nishi *et al.*<sup>31</sup> are only used to fit the thresholds and white lines of the spectra, but they cannot reproduce the multiple scattering region of the XANES trace, where an important part of the stereochemical information is observed.

The XANES spectra of the “as-prepared” GaGe-ZEOL and GaAl-ZEOL samples are shifted to lower energies with respect to the thermally treated samples. Moreover, the feature at 10379.5 eV can be easily observed in both “as-prepared” samples. These two facts are in agreement with tetrahedral coordination for the Ga atoms in the “as-prepared” samples and a mixed coordination (tetrahedral and octahedral) after the thermal treatment. In order to demonstrate this, Fig. 4(a) present a comparison between the  $\beta$ -Ga<sub>2</sub>O<sub>3</sub> XANES spectrum and a linear combination of the spectra corresponding to  $\alpha$ -Ga<sub>2</sub>O<sub>3</sub> and the untreated GaGe-ZEOL sample, with a weight of one half for each.

The XANES spectra of the calcined and dehydrated GaGe-ZEOL and GaAl-ZEOL samples can be simulated by a linear combination of the “as-prepared” (tetra) and the  $\alpha$ -Ga<sub>2</sub>O<sub>3</sub> (octa) XANES spectra. The best fits are shown in Fig. 4 and the relative percentages obtained are given in the last column of Table 1.

The XANES results are in agreement with those from EXAFS and can be rationalized as follows: “as-prepared” samples have Ga atoms in the Beta zeolite skeleton sites. After calcination of the GaGe-ZEOL and GaAl-ZEOL samples, nearly 45% of the Ga atoms are found to have moved from the Beta zeolite skeleton to octahedral “extra-framework” positions. Dehydration induces a smaller percentage of “extra-framework” migrations (25%).

It should be noted that the method used to obtain the relative tetrahedral and octahedral percentages by fitting the XANES spectra is independent of the number of structural defects. This independence is in contrast with the percentages that can be

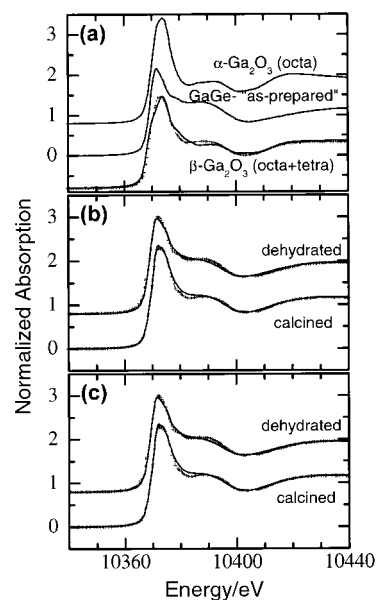


**Fig. 4** (a) XANES spectra of  $\alpha$ -Ga<sub>2</sub>O<sub>3</sub>, “as-prepared” GaGe-ZEOL and the fit of the  $\beta$ -Ga<sub>2</sub>O<sub>3</sub> sample spectrum. (b) Fit of the calcined and dehydrated GaGe-ZEOL samples. (c) Fit of the calcined and dehydrated GaAl-ZEOL samples. Continuous lines are the experimental spectra and crosses are obtained by linear combination of  $\alpha$ -Ga<sub>2</sub>O<sub>3</sub> and “as-prepared” sample spectra.

obtained from the coordination numbers resulting from the EXAFS analysis. Nevertheless, it is clear that the defect structure should be different for the GaGe- and GaAl-zeolites because the percentages obtained by XANES are identical for the calcined and dehydrated samples but the coordination numbers obtained by EXAFS are slightly different.

## IV Conclusions

EXAFS and XANES spectroscopies have proved that Ga is incorporated into the Beta zeolite. “As-prepared” samples have Ga atoms in zeolite skeleton sites. The corresponding tetrahedrally coordinated oxygens are at a distance of 1.80 Å. Upon calcination of the GaGe-ZEOL sample, nearly 45% of the Ga atoms move from the Beta zeolite skeleton to octahedral (“extra-framework”) positions with two different Ga–O distances of 1.83 and 1.94 Å. Dehydration does not change the distances, but induces a lower percentage of extra-framework migrations (25%). Similar behavior is observed for the GaAl-ZEOL sample. After calcination, the obtained distances for the 45% of the Ga atoms in octahedral positions are 1.75 and 2.03 Å, which suggests that the GaO<sub>6</sub> octahedra are more distorted than in the “as-prepared” sample. Octahedral coordination has also been found for 25% of the Ga atoms in the dehydrated GaAl-ZEOL sample. Recently, Lamberti *et al.*<sup>32</sup> have obtained similar conclusions in the parent Ga-MFI system by analyzing EXAFS data.

## Acknowledgements

We acknowledge the staff in charge of the DCI storage ring of LURE for beam time allocation, special thanks are given to Dr. F. Villain for experimental assistance. This work has been partially supported by Spanish CICYT under contract MAT97/0725.

## References

- 1 A. Yu. Khodakov, L. M. Kustov, T. N. Bondarenko, A. A. Dergachev, V. B. Kazansky, Kh. M. Minachev, G. Gorbely and H. K. Beyer, *Zeolites*, 1990, **10**, 603.

- 2 G. P. Handreck and T. D. Smith, *J. Catal.*, 1990, **123**, 513.
- 3 D. K. Simmons, R. Szostak, P. K. Agrawal and T. L. Thomas, *J. Catal.*, 1987, **106**, 287.
- 4 J. Kanai and N. Kawata, *Appl. Catal.*, 1989, **55**, 115.
- 5 J. M. Newsam, M. M. Treacy, W. T. Koetsier and C. B. de Gruyter, *Proc. R. Soc. London A*, 1988, **420**, 375.
- 6 M. Taramasso, G. Perego and B. Notari, *US Patent No.* 4 656 016, 1987.
- 7 M. A. Cambor, J. Pérez-Pariente and V. Fornés, *Zeolites*, 1992, **12**, 280.
- 8 M. A. Cambor, A. Corma and J. Pérez-Pariente, *Zeolites*, 1993, **13**, 82.
- 9 J. M. Thomas and X. Liu, *J. Phys. Chem.*, 1986, **90**, 4843.
- 10 V. R. Choudhary, C. Sivadinarayana and A. K. Kinage, *J. Catal.*, 1998, **173**, 243.
- 11 C. R. Bayanse, A. P. M. Kentgens, J. W. de Haan, L. J. M. van de Veen and J. H. C. van Hooff, *J. Phys. Chem.*, 1992, **96**, 775.
- 12 H. Kosslick, V. A. Tuan, B. Parlitz, R. Fricke, C. Peuker and W. Storek, *J. Chem. Soc., Faraday Trans.*, 1993, **89**, 1131.
- 13 E. Lalik, X. Liu and J. Klinowski, *J. Phys. Chem.*, 1992, **92**, 805.
- 14 C. Otero-Areán, G. Turnes-Palomino, F. Geobaldo and A. Zecchina, *J. Phys. Chem.*, 1996, **100**, 6678.
- 15 T. Blasco, M. A. Cambor, A. Corma and J. Pérez-Pariente, *J. Am. Chem. Soc.*, 1993, **115**, 11806.
- 16 M. H. Tuilier, *Zeolites*, 1991, **11**, 662.
- 17 P. Behrens, *Catal. Today*, 1991, **8**, 479.
- 18 S. A. Axon, K. Huddersman and J. Klinowski, *Chem. Phys. Lett.*, 1990, **172**, 398.
- 19 D. Bonnin, P. Kaiser and J. Desbarres, EXAFS PC-software, 8th Europhys. School on Chemical Physics, La Rabida, 1992.
- 20 See for instance: D. C. Koningsberger and R. Prins, *X-Ray Absorption Principles, Applications, Techniques of EXAFS, SEXAFS and XANES*, Wiley, New York, 1988.
- 21 J. J. Rehr, S. I. Zabinsky and R. C. Albers, *Phys. Rev. Lett.*, 1992, **69**, 3397.
- 22 M. Marezio and J. P. Remeika, *J. Chem. Phys.*, 1967, **46**, 1862; M. Marezio and J. P. Remeika, *Struct. Rep.*, 1967, **32A**, 257.
- 23 J. J. Rehr, *Jpn. J. Appl. Phys.*, 1993, **32**, 8.
- 24 S. Geller, *J. Chem. Phys.*, 1960, **33**, 676; J. A. Kohn, G. Katz and J. D. Broder, *Am. Mineral.*, 1957, **42**, 398; J. A. Kohn, G. Katz and J. D. Broder, *Struct. Rep.*, 1957, **21**, 219.
- 25 E. Stern, D. Sayers and F. Lytle, in *X-Ray Absorption Fine Structure*, ed. S. S. Hasnain, Harwood, Chichester, 1991, p. 751.
- 26 J. M. Newsam and J. D. Jorgensen, *Zeolites*, 1987, **7**, 569.
- 27 P. Behrens, H. Kosslick, V. A. Tuan, M. A. Fröba and F. Neissendorfer, *Microporous Mater.*, 1995, **3**, 433.
- 28 J. P. Itié, A. Polian, G. Calas, J. Petiau, A. Fontaine and H. Tolentino, *Phys. Rev. Lett.*, 1989, **63**, 398.
- 29 D. Andrault, M. Madon, J. P. Itié and A. Fontaine, *Phys. Chem. Miner.*, 1992, **18**, 506.
- 30 P. E. Petit, F. Guyot, G. Fiquet and J. P. Itié, *Phys. Chem. Miner.*, 1996, **23**, 173.
- 31 K. Nishi, K. Shimizu, M. Takamatsu, H. Yoshida, A. Satsuma, T. Tanaka, S. Yoshida and T. Hattori, *J. Phys. Chem. B*, 1998, **102**, 10190.
- 32 C. Lamberti, G. Turnes-Palomino, S. Bordiga, A. Zecchina, G. Spanò and C. Otero-Areán, *Catal. Lett.*, 1999, **63**, 213.